3D spatial resolution evaluation for helical CT according to ASTM E1695 – 95

Jakub Laznovsky[1], Adam Brinek[1], Jakub Salplachta[1], Tomas Zikmund[1], Ben Young[2], Zuzana Patákova[2], Jozef Kaiser[1]

[1]Central European Institute of Technology, Brno University of Technology, 616 00 Brno, Czech Republic, e-mail: jakub.laznovsky@ceitec.vutbr.cz, adam.brinek@ceitec.vutbr.cz, jakub.salplachta@ceitec.vutbr.cz, tomas.zikmund@ceitec.vutbr.cz, jozef.kaiser@ceitec.vutbr.cz,

[2]ThermoFisher, Vlastimila Pecha 12, Brno, Czech Republic, e-mail: ben.young@thermofisher.com, zuzana.patakova@thermofisher.com

Abstract

Knowledge of valid spatial resolution is essential for quantitative analysis using X-ray computed tomography. Due to the spatial resolution, it is possible to determine with what detectability the imaging system can measure an internal structure**.** Based on the spatial resolution knowledge, the smallest object size that can be distinguished in resulting images can be determined. Each component in the imaging system affects the value of spatial resolution, and the final value is defined as a product of all comprised components. In this paper, spatial resolution according to standard ASTM E1695 – 95 was calculated. This standard uses edge response function (ERF), point spread function (PSF) to modulation transfer function (MTF) approach for the calculation of spatial resolution in each plane. For the calculation was used a sphere phantom, which is convenient for the study of spatial resolution in all three orthogonal planes. Spatial resolution was tested on spheres from two different materials, to observe the effect of material on spatial resolution in all three dimensions.

Keywords: X-ray computed tomography, Helical CT, Spatial resolution, Space filling, self calibrated system

1 Introduction

The X-ray computed tomography (XCT) has been found to provide excellent three dimensional (3D) sample characterisation in the millimetres to micrometres scale [1]. This method uses the X-ray beam that penetrates the sample and its attenuation is detected. The value of attenuation is given by a density of the materials included in a sample. The basic principle of obtaining final XCT dataset is a measurement of many projections in various angles. The measured X-ray projections are then reconstructed and 3D data are visualised as cross sections through the sample [2].

In general, there are two traditional ways of industrial/laboratory XCT systems constructions. The first system has a stationary X-ray source and sample rotates during the measurement. The second system also has a stable X-ray source with detector but the sample is rotating and also moving up or down. Introduced trajectories are called circular and helical respectively. These trajectories have a different impact on image quality [1].

The circular trajectory has advantages in the scanning of the samples with similar sizes in all directions. The helical trajectory helps in the case of scanning the long sample with one size bigger then detector width. In the case of the helical trajectory, the scanning time of such a sample is shortened. Another advantage is reducing artefacts influencing the grey value homogeneity within one material. The most significant advantage is the quality of the top sample surface. Top surface or top area of reconstructed images is frequently used for correlation with other imaging techniques. Different artefacts have a significant influence on this part [1].

Spatial resolution is one of the significant characteristics of CT systems. The resolution itself means the ability to distinguish spatial details without blur. Based on spatial resolution, a smallest visible object in reconstructed images can be determined. Many methods are providing the measurement of spatial resolution. 1) Measurement of point spread function based on ball or wire – using the reconstructed image of a point source. 2) Edge methods – Spatial resolution determination is based on line profile in one particular row or column that is crossing the imaged of the edge (e.g., Slanted edge method or edge of circular phantom made from uniform material). 3) Measurement in the scale of spatial frequencies – phantoms using line pairs, over which is a line profile crossed. These phantoms are commercially available, but limiting resolution always falls between fixed frequencies [3].

The exact spatial resolution in 3D depends on many factors, not only on the mechanical accuracy of the system. The required temporal stability during the scan is much more demanding than the relatively short duration of 2D tests. Also, the processing and reconstruction algorithms have a significant influence on the achievable spatial resolution in 3D. Two main factors affecting the quality of a CT image are geometrical unsharpness and random noise. Geometrical unsharpness limits the spatial resolution of a CT system, that is, its ability to image fine structural detail in an object. Random noise limits the contrast sensitivity of a CT system, that is, its ability to detect the presence or absence of features in an object. Spatial resolution and contrast sensitivity may be measured in various ways. ASTM specifies spatial resolution is quantified in terms of the MTF and contrast sensitivity be quantified in terms of the contrast discrimination function (CDF) (see Guide E 1441 and Practice E 1570). This test method allows the purchaser or the provider of CT systems or services, or both, to measure and specify the spatial resolution and contrast sensitivity.

For obtaining the exact 3D spatial resolution, we utilised the X-ray tomographic system Heliscan, the product of Thermo Fisher Scientific. It is a self-calibrated system, utilising modified autofocus function for estimation of the relevant parameters of acquisition trajectory. There is also a PCM function for motion reduction, applied during the reconstruction process. Thanks to these algorithms, this system allows providing high-resolution, theoretically-exact tomographic reconstruction [4].

In this paper, the 3D spatial resolution was observed with helical and circular trajectory. For the observation was used a ball phantom convenient for computation of spatial resolution based on edge response. The spatial resolution could be calculated from the edge response according to the proposed algorithm.

2 Materials and methods

2.1 Modulation transfer function

In the proposed approach, spatial resolution calculation is based on the quantitative measurement of the MTF. MTF relates the spatial frequency of sample features to the corresponding loss of contrast in their image [5].

In this study, 3D spatial resolution is considered as a particular spatial resolution in individual orthogonal cutting planes. Thanks to this approach, we can observe and compare the dependence of the sample placed in the system to the spatial resolution. As a result, three numbers are characterising spatial resolution for each orthogonal plane. Entire spatial resolution can be characterised as a mean value of individual spatial resolutions in each plane (see eq.1).

$$\boldsymbol{SR_E} = \frac{1}{3}\sum_{k=1}^{3} \boldsymbol{x_k} \tag{1}$$

where SR_E is the spatial resolution of the system and k corresponds to original spatial resolution in each cutting plane.

The Fourier-based analytical approach was developed to accurately characterise the spatial resolution and MTF for the entire frequency range. The algorithm is based on the determination of MTF from edge response function (ESF), the Fourier transform of it is the first derivative finally provides several values of the wanted MTF. The relation is given by

$$MTF(k_x) = F\left\{\frac{d}{dx}ESF(x)\right\},$$

where kx is the spatial frequency in the x-direction. This formula is more described in [3]

2.2 Phantom design

Ball phantom was designed for determination of spatial resolution. The material type comply mentioned ASTM standard suitable for this study. The ceramic ball is manufactured with high precision and minimal surface roughness (Grade 25). The phantom consist of a ball glued to a carbon bar. Despite [7] indicate that the rod should be used, the ball phantom is more promising when the 3D resolution should be achieved. The rod enables the analysis only in the parallel cross section to the beam. The ball phantom was chosen for the reason that the orthogonal cross sections can be easily achieved.

From the whole volume of the ball, three slices were chosen in every plane (transversal, coronal, sagittal) approximately crossing the middle of the ball. For each of these slices, the value of spatial resolution will be calculated. The average value of these three MTF values corresponds to the 3D spatial resolution of the scanner.

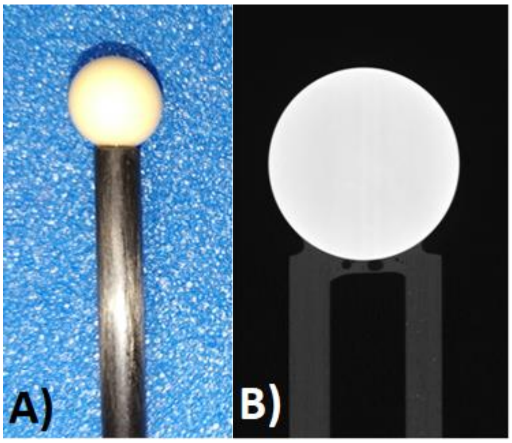

Figure 1: The photo of the ceramic ball glued on the plastic rod A). The cross section of the phantom B).

2.3 Acquisition

The phantom was scanned on Heliscan, the product of Thermo Fisher Scientific. Heliscan uses helical trajectory measurement technique called Space Filling [4], [5]. Micro CT HeliScan MK1 scanned the ceramic ball with 2.3 µm linear voxel size. The scans were performed with X-ray tube 20 – 160 kV up to 300 µA with a tungsten target and wide cone angle ~ 160°. The high contrast detector 3000 × 3000 px with 139 µm. The exposure time was 2 × 0.6 s in each of the 2880 projections per evolution. In all measurement, the utilised acceleration voltage and X-ray current were 100 kV and 160 µA, respectively. The beam was filtered with 0.22 mm of stainless steel.

The tomographic reconstruction was realised using Thermo Fisher Scientific reconstruction software with correction on sample drift and beam hardening. The Autofocus function was used to align the projections for iterative reconstruction. Reconstructions were performed on a 4-node cluster. The total reconstructed volume was 39x39x41 mm.

Two scans were provided one measurement of the phantom with Space filling trajectory and one measurement of the phantom with circular trajectory. Both measurements were performed with the same parameters.

3 Results and discussion

The main focus of this paper is in the method for achieving the 3D spatial resolution. The method is following the ASTM E1695 – 95. Helical scan results of ceramic ball phantom are described below.

The whole calculation process was done in Python programming language. At first, phantom material has to be detected. For this purpose, the Hough transform for detecting circles was utilised. The result of the fitting circles is in the fig. 1. This method proved very convenient due to high accuracy for precisely spherical shape. If the shape of the reconstructed phantom is little inaccurate and does not have a strictly spherical shape, the boundary circles are also detected. However, irregular boundaries for determining the area of calculations will negatively affect the resulting spatial resolution, which is suitable for detecting reconstruction inaccuracies.

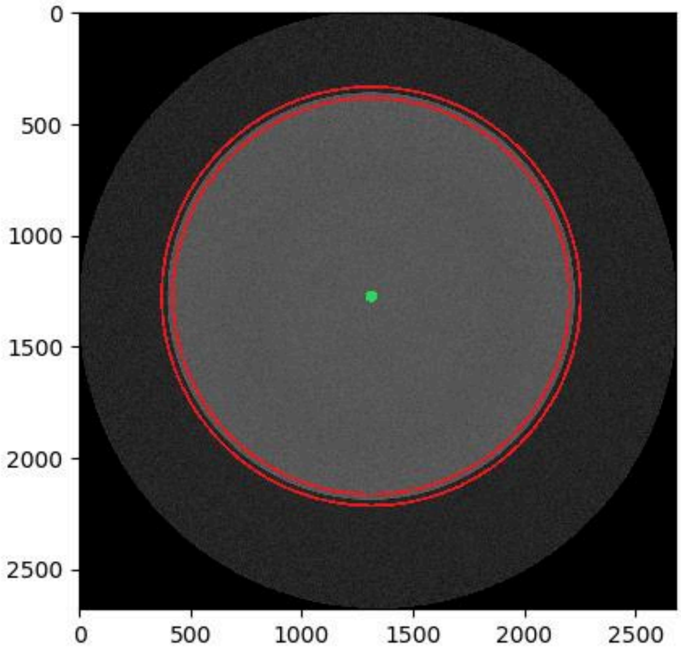

Figure 1: Measured ball phantom depicted in xy plane. Green point – the estimated centre of mass. The area enclosed by two red circles enters the calculation process

In the next step, all pixels corresponding to the restricted area are extracted in the dependence to the centre of mass. Afterwards, individual pixels are segregated into bins (ERF with binned pixels in fig. 3 A). Bin size is chosen as small as possible, avoiding empty bins. The number of bins depends on the area covered by the material, but there are approximately 1500 bins per single measurement. Size of one bin corresponds to 0.04 pixel size. Due to a large number of pixels involved in the analysis (approx. 300 000) can be bin size so small which enhances a statistical relevance. This approach ensures obtaining ERF. For obtaining PSF of the system, the smoothing of the ERF is crucial (fig. 3 B).

The smoothing is accomplished iteratively using piece-wise, least-squares cubic fit an specified number of ERF values and replacing the middle value with that predicted by the fit. The PSF value corresponding to the middle of each window is obtained applying the same iterative piece-wise, least-squares cubic fit to already smoothed ERF and computing the analytical derivative of a resultant polynomial,

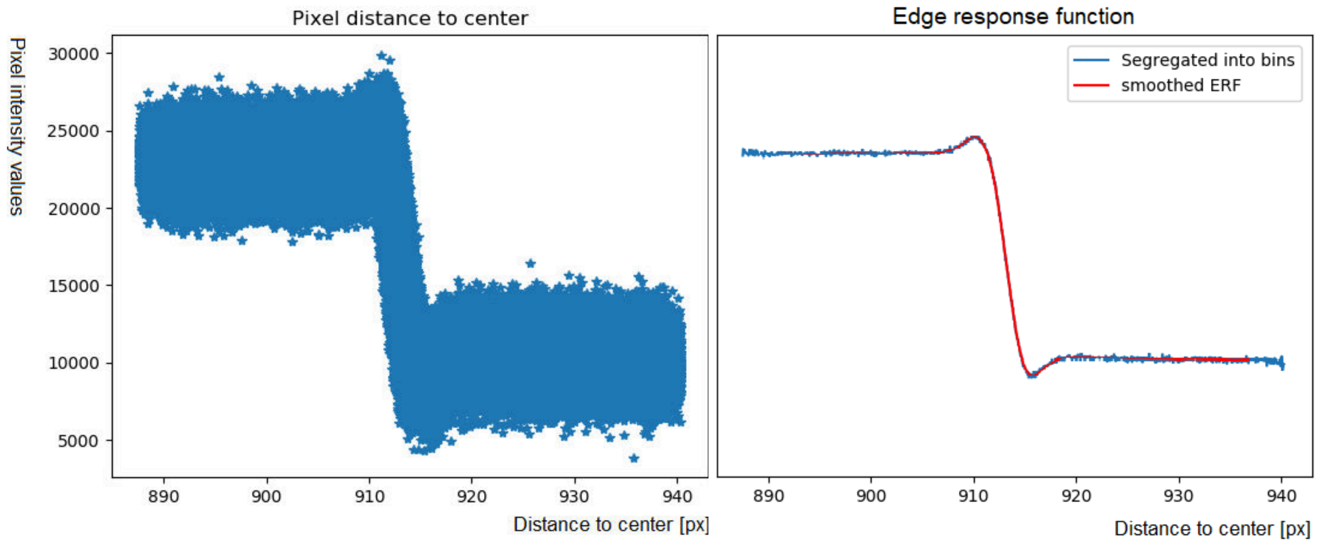

Figure 3: The resulting ERF for the presented method A). The ERF after segregation into the bins and least-square cubic fit B).

The resulting PSF curve is depicted as the function of distance from the centre of the disc and normalised to <0;1> interval along the y-axis (calculated PSF from ERF fig. 4 A). The resulting spatial resolution is derived from MTF, and it is calculated as a Fourier Transform of PSF. Cropped PSF is used for MTF calculation (fig. 4 B). Sampling frequency for calculation of Fourier Transform is 0.01, which ensures that the resulting MTF curve is smooth enough and all values of PSF are included.

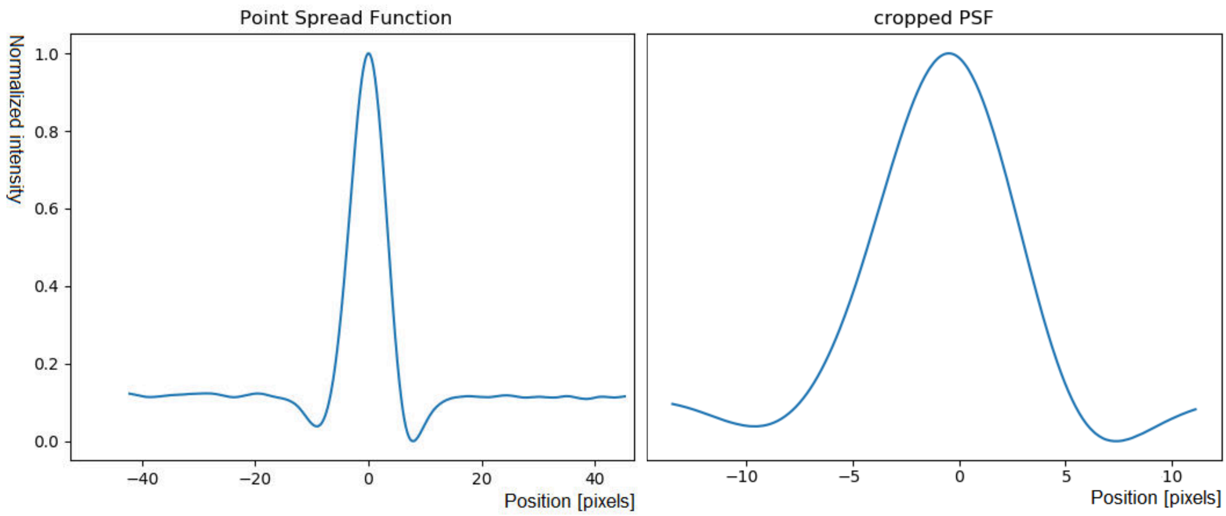

Figure 4: PSF function achieved from smoothed ERF A). Cropped PSF function which was used for relevant MTF calculation B).

The MTFs in the three planes are different since the focal spot shape and the actual spatial resolution distribution in 3D space will affect the results. Resulting MTF is in figure 5. The conventional resolution is calculated in 1/10 % of the MTF. The resulting spatial resolutions for individual cross sections are in the tab. 1.

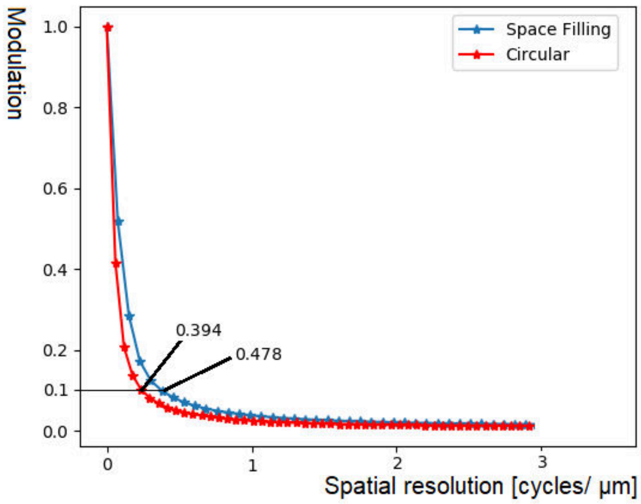

Figure 5: Resulting MTF for the ceramic ball phantom and helical space filling trajectory.

The main difference in the results between the circular and helical trajectory lies in the cross section parallel with the X-rays. The spatial resolution results are in the magnitude of the voxel size. This fact can be explained in a way that the ceramic ball has very high density against the air. Also, the noise is reduced due to the averaging of the projections. Thus the signal to noise ratio and so the detectability of the ceramic material in the images is very high. The differences between the cross sections in other directions are small and minor. The final 3D spatial resolution of the system for the presented phantom for the scan with circular and helical trajectory are 4.701 ± 0.235 and 4.039 ± 0.202, respectively.

Table 1: Results of the spatial resolution in 10 % of MTF calculated from the cropped PSF.

Measurement:	Circular [µm]	Space filling [µm]
XY plane	2.536	2.090
XZ plane	6.110	5.531
YZ plane	5.456	4.498
3D	4.701	4.039

However, these methods are still more suitable for the fan-beam CT system but it can also be used for the cone-beam CT system. In the cone-beam system, obtaining the 3D PSF can lead to better characterisation of the spatial resolution and the accuracy can increase. Despite this, the measured spatial resolution and MTF calculation are accurate within ± 5 % and it can also be repeated with the ± 5 % according to [7].

The biggest challenge on the way to a proper MTF from the edge response function of the presented phantom is the determination of the balls centre with very high accuracy. If the centre is not defined correctly, the binning of the pixels according to the centre will not be accurate and the error will result in the blurred edge.

The ball division into the small segments is possible improvements for the future. The MTF can be calculated in all of these segments and the 3D spatial resolution can be studied for more directions. Also, calculation of 3D PSF is possible with the presented approach and it can be in the future interest to calculate the 3D PSF and so to understand the detectability in the sample. Furthermore, shown approach and presented phantom can be used to calculate the contrast discrimination function (CDF). CDF is in particular interest in the detectability studies.

3 Conclusions

The phantom consisting of carbon stick and the ceramic ball was designed based on ASTM E1695 – 95. CT measurements of the phantom with Space Filling and circular trajectory were performed. From every dataset, three slices corresponding to individual three cutting planes were chosen. Corresponding MTFs and appropriate spatial resolution were calculated based on these three slices. All calculations were done in Python programming environment. The value of 3D spatial resolution was computed as an average of spatial resolutions in all three planes for the corresponding dataset. The resulting spatial resolution of the scan with circular and helical trajectory are 4.701 ± 0.235 and 4.039 ± 0.202, respectively.

Acknowledgements

This research was carried out with financial support TA ČR (project TN01000008) and under the project CEITEC 2020 (LQ1601) with financial support from the Ministry of Education, Youth and Sports of the Czech Republic under the National Sustainability Programme II and support of CEITEC Nano Research Infrastructure (MEYS CR, 2016–2019).

References

[1] S. Stock. Microcomputed tomography: methodology and applications. Boca Raton: CRC Press, 2009. ISBN 978- 142-0058-765.

[2] A. Břínek, J. Lázňovský, T. Zikmund, J. Šalplachta, J. Kaiser. Helical XCT measurement for correlative imaging. ICT2019 [online]. , 1-6. Available: https://www.ndt.net/article/ctc2019/papers/iCT2019_Full_paper_89.pdf

[3] SAMEI, Ehsan, M. J. Flynn, D. A. Reimann. A method for measuring the presampled MTF of digital radiographic systems using an edge test device. Medical Physics [online]. 1998, 25(1), 102-113 [cit. 2019-11-13]. DOI: 10.1118/1.598165. ISSN 00942405. Available: http://doi.wiley.com/10.1118/1.598165

[4] T. Varslot, A. Kngston, G. Myers, A. Sheppard. High-resolution helical cone-beam micro-CT with theoretically-exact reconstruction from experimental data. Medical Physics [online]. 2011, 38(10), 5459-5476 [cit. 2019-11-13]. DOI: 10.1118/1.3633900. ISSN 00942405. Dostupné z: http://doi.wiley.com/10.1118/1.3633900

[5] A. M. Kingston, G. R. Myers, S. J. Latham, B. Recur, H. Li, A. P. Sheppard. Space-Filling X-Ray Source Trajectories for Efficient Scanning in Large-Angle Cone-Beam Computed Tomography. IEEE Transactions on Computational Imaging [online]. 2018, 4(3), 447-458. DOI: 10.1109/TCI.2018.2841202. ISSN 2333-9403. Available: https://ieeexplore.ieee.org/document/8367874/

[6] J. Rueckel, M. Stockmar, F. Pfeiffer, J. Herzen. Spatial resolution characterization of a X-ray microCT system. Applied Radiation and Isotopes [online]. 2014, 94, 230-234 [cit. 2019-11-13]. DOI: 10.1016/j.apradiso.2014.08.014. ISSN 09698043. Available: https://linkinghub.elsevier.com/retrieve/pii/S0969804314003157

[7] Standard Test Method for Measurement of Computed Tomography (CT) System Performance: E 1695 – 95. 1st edition. United States: American Society for Testing and Materials, 2013